frontiers | Frontiers in Chemical Engineering

TYPE Original Research
PUBLISHED 04 March 2025
DOI 10.3389/fceng.2025.1532958

OPEN ACCESS

EDITED BY
Chang Geun Yoo,
SUNY College of Environmental Science and Forestry, United States

REVIEWED BY
Ankita Juneja,
University of Illinois at Urbana-Champaign, United States
Yunxuan Wang,
The University of Tennessee, Knoxville, United States

*CORRESPONDENCE
Belinda S. M. Sturm,
bmcswain@ku.edu

RECEIVED 22 November 2024
ACCEPTED 14 February 2025
PUBLISHED 04 March 2025

CITATION
Romero AD, Poli JV, Larson S, Stagg-Williams S, Carter R and Sturm BSM (2025) Inhibition of nitrifying bacteria from heterocyclic N-containing organic compounds from municipal sludge hydrothermal liquefaction.
Front. Chem. Eng. 7:1532958.
doi: 10.3389/fceng.2025.1532958

Inhibition of nitrifying bacteria from heterocyclic N-containing organic compounds from municipal sludge hydrothermal liquefaction

Adrian D. Romero[1], João V. Poli[2], Sean Larson[2], Susan Stagg-Williams[2], Ray Carter[1] and Belinda S. M. Sturm[1]*

[1]Department of Civil, Environmental and Architectural Engineering, University of Kansas, Lawrence, KS, United States, [2]Department of Chemical and Petroleum Engineering, University of Kansas, Lawrence, KS, United States

Hydrothermal liquefaction (HTL) is a thermochemical technology that converts wet biomass into biochar and biocrude at high temperatures and pressures. HTL can be utilized within municipal wastewater treatment to convert waste activated sludge (WAS) into valuable resources, but HTL by-products include an aqueous coproduct (ACP) that has been characterized for its biological toxicity, high ammonia, and presence of heterocyclic N-containing organic compounds (HNOCs). This study evaluated the inhibitory effects of the most prevalent HNOCs on autotrophic nitrifiers present in WAS, by determining the concentration that reduces ammonia uptake by 50 percent (IC_{50}). 2-pyrrolidinone, pyrazine, and 2- piperidinone and their derivatives were the most prevalent HNOCs in ACP from WAS at concentrations of 8.98, 6.05, and 0.40 mM respectively. The IC_{50} of 2-pyrrolidinone and pyrazine were 5.2×10^{-5} and 2.0×10^{-3} mM, respectively. The IC_{50} of the ACP was 0.08% (%v/v). This corresponded to concentrations of 2- pyrrolidinone, pyrazine, and 2-piperidinone of 7.52×10^{-3}, 5.07×10^{-3}, and 3.36×10^{-4} mM, respectively. The impact of ACP storage was also tested. ACP stored for 15 weeks exhibited less inhibitory effects on the nitrifying community compared to ACP stored for 1 week. The % maximum ammonia uptake rate was reduced by 23% for the 15-week stored ACP, in contrast to 51% reduction for ACP stored for 1 week. Results of this study provide guidance for how ACP recycle can be incorporated at a wastewater treatment plant without inhibiting nitrification, enhancing the feasibility of using HTL as a solids processing technology.

KEYWORDS

hydrothermal liquefaction, aqueous co-product, nitrifying bacteria, municipal sludge, inhibition, recycle

Abbreviations: ACP, Aqueous Co-Product; AOB, Ammonia Oxidizing Bacteria; DCM, Dichloromethane; GC-MS, Gas Chromatography - Mass Spectrometry; HNOC, Heterocyclic N-containing Organic Compounds; HTL, Hydrothermal Liquefaction; IC_{50}, Half-Maximum Inhibitory Concentration; KRWWTP, Kansas River Wastewater Treatment Plant; MLVSS, Mixed Liquo Volatile Suspended Solids; NOB, Nitrite Oxidizing Bacteria; POTW, Publicly Owned Treatment Works; RAS, Return Activated Sludge; SAUR, Specific Ammonia Uptake Rate; sCOD, soluble Chemical Oxygen Demand; SPE, Solid-Phase Extraction; VFA, Volatile Fatty Acids; VSS, Volatile Suspended Solids; WAS, Waste Activated Sludge.

Introduction

Municipal wastewater treatment utilizes biological treatment that produces waste activated sludge (WAS), which must be disposed of in an economically- and environmentally responsible fashion. Within the United States, publicly owned treatment works (POTWs) process 34.5 Bgal/d of wastewater, which generates millions of tons of sludge (Tarallo, 2014). The treatment and disposal of sludge is an economic burden requiring $300-$800 per ton, but there is potential to reduce these costs and recover chemical energy, nutrient, and metal assets valued at approximately $550 per ton l (Peccia and Westerhoff, 2015). A common treatment approach for WAS is anaerobic digestion, but this is inefficient in terms of materials recovery (Mulchandani and Westerhoff, 2016; Rittmann et al., 2011), and chemical energy can be lost through biogas flaring. The resulting stabilized biosolids may be land applied in the United States, but there are concerns for microplastic and PFAS leaching that may hinder biosolids application in the future, highlighting the need for alternative processes to treat stabilize sludge and recover resources from this waste material.

Municipal sludge can serve as a rich biomass feedstock to produce high-value products. Hydrothermal liquefaction (HTL) is a promising technology developed for energy recovery from municipal sludge and other biomass feedstocks like microalgae and/or food waste (Wu et al., 2020). HTL consists of a high-pressure, high-temperature reaction to convert organic solids in high moisture into liquid fuel products (e.g., biocrude), a solid residue (biochar), gas, and water-soluble products. The typical reaction temperatures can vary between 200°C and 375°C and pressures up to 22 MPa (Wu et al., 2020). HTL is advantageous compared to other thermochemical conversions as it utilizes a wet feedstock and avoids drying costs. The purpose of conducting HTL on waste activated sludge is to produce biocrude from a renewable source while minimizing sludge stabilization costs associated with conventional technologies like anaerobic digestion. Furthermore, HTL can be incorporated with other technologies to optimize the recovery of nutrients like N & P (Li et al., 2018). Even though the main product from HTL is the biocrude, the other products must be assessed when considering this technology.

HTL accumulates nitrogen in the aqueous phase and phosphorus in the solid biochar product phase (Watson et al., 2020; Hable et al., 2019). The aqueous co-product (ACP) contains high concentrations of volatile fatty acids (VFAs) (10–17 g/L), total ammonia (3.9–7.1 g/L), dissolved proteins (10–20 g/L), total phenols, and heterocyclic N-containing organic compounds (HNOCs) (Basar et al., 2023; Wu et al., 2020). HNOCs are organic compounds with a ring structure with at least one carbon and nitrogen attached. Pham et al. identified 48 organic compounds that are commonly reported in HTL wastewater including many HNOCs (Pham et al., 2013). These can be classified by their ring structures (typically 5 or 6-membered chains), saturation status, and whether they are aromatic or non-aromatic. HNOC toxicity to bacteria and mammalian cells has been reported (Zhou et al., 2018; Pham et al., 2013; Padoley et al., 2008; He et al., 2017). In one study, more diverse HNOCs and higher concentrations of non-biodegradable organic nitrogen were associated with greater toxicity for heterotrophic bacteria *Bacillus subtilis* and *Pseudomonas putida* (Alimoradi et al., 2020). Some HNOCs are known to inhibit autotrophic nitrifiers as well, although these have been mainly studied in soil systems (Papadopoulou et al., 2020; Beeckman et al., 2023; Hayden et al., 2021).

For HTL to be integrated into a municipal wastewater treatment, the aqueous product of HTL will need to be treated. There are various investigations on ACP treatment through wet oxidation, anaerobic digestion, utilization of nitrogen for algal growth, and gasification (Gu et al., 2019; Li et al., 2022; Adedeji et al., 2023; Thomsen et al., 2022; Chen et al., 2020; Xu et al., 2019). Despite this research, a practical method for full-scale application was not determined due to the complex nature and unknown toxicity of the compounds within the ACP. For many sludge stabilization technologies, such as anaerobic digestion or thermal hydrolysis, ammonia-rich centrate from these processes is recycled to the activated sludge basins for biological treatment. A schematic of ACP recycle is shown in Figure 1. Previous research focused on determining the HNOC toxicity on heterotrophic bacterial growth from microalgae-derived HTL wastewater (Alimoradi et al., 2020; Roberts et al., 2013). When considering recycling ACP into an aerobic activated sludge basin, potential inhibition to autotrophic nitrifiers must be studied, since this community is slow-growing, and nitrifiers are necessary for ammonia removal.

The objective of this study is to determine the inhibitory effects of predominant HNOCs within ACP from municipal sludge HTL on nitrifying bacteria, because nitrifier growth and ammonia oxidation are typically rate-limiting for activated sludge treatment. ACP was generated from municipal sludge, and the predominant HNOCs were identified and tested individually and as a mixture. Inhibition of nitrification was determined using batch ammonia uptake rate assays using a nitrifying activated sludge from a full-scale wastewater treatment plant. This study will help determine the feasibility of recycling the aqueous stream into the wastewater liquid train without causing adverse impacts on the biological treatment process. The study will provide better understanding towards ACP management strategies when incorporating HTL as a solids treatment technology and is the first to show inhibitory effects of specific HNOC compounds and ACP to nitrifying communities.

Materials and methods

Municipal sludge collection and HTL reaction setup

Waste Activated Sludge (WAS) was collected from the Kansas River Wastewater Treatment Plant (KRWWTP), located in Lawrence, Kansas, United States with an approximate sample volume of 20 L. Following collection, the WAS suspensions were centrifuged at 3000 RPM for 15 min, and the wastewater supernatant was reserved from this step. The pelleted sludge was dried overnight at 105°C. The dried sludge solids were homogenized using a standard coffee grinder before HTL.

HTL reactions were conducted in 75 mL, 4,740 series Parr reactors. The reactors were loaded with samples containing 10 wt.% solids, in addition to 30 mL of wastewater previously separated in the centrifugation step. Prior to heating, the reactors were purged with N_2 and then placed in a Techne SBL-2D fluidized

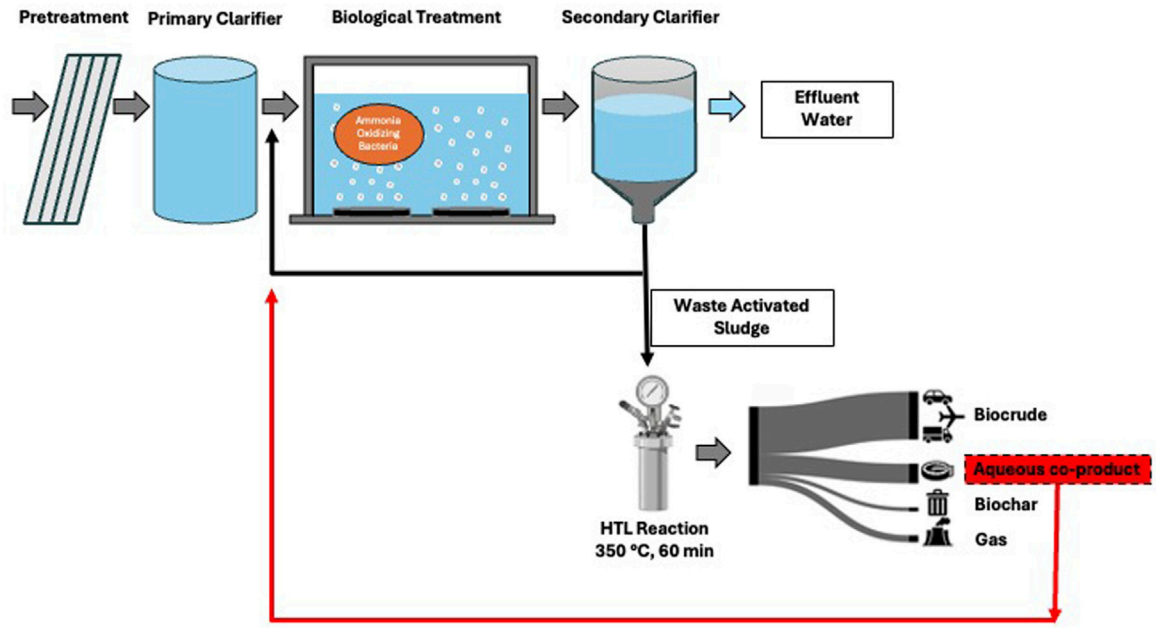

FIGURE 1
Process flow diagram of how HTL can be implemented at a municipal WWTP to convert waste activated sludge to biocrude and biochar. The aqueous co-product would be recycled to the biological treatment train, where the activity of ammonia oxidizing bacteria is necessary for nitrification and ammonia removal.

sand bath with a Techne TC-8D temperature controller at room temperature. The sand bath's temperature was set to 350°C and held isothermally for 1 hour. After the reaction, the reactor vessels were directly quenched in room-temperature water for 5 min. After cooling, the contents of the reactors were transferred to glass centrifuge tubes and centrifuged at 5000 RPM for 10 min. The supernatant was vacuum filtered using a pre-rinsed GF/F Whatman glass-fiber filter paper with 0.7 µm pore diameter, and the collected ACP volume was recorded. Biocrude and biochar remaining in the reactors were separated and preserved for further analysis. ACP was stored for 1 week and for 15 weeks before extracting HNOCs using liquid-liquid extraction.

Liquid-liquid extraction of HNOCs

10 mL of ACP was added to a separatory funnel, and the pH was raised to 14 through addition of 5M KOH. 10 mL of dichloromethane (DCM) was added to the funnel, shaken for 2 min to extract the HNOCs, and allowed to separate 10 min, and the DCM layer was collected as the first extract. The supernatant was acidified to a pH of 5 with 5M HCl. 10 mL of DCM was added and the funnel was shaken for 2 min. The DCM layer was collected as the second extract. Lastly, a solid-phase extraction (SPE) was performed on the recovered supernatant from the second extraction using a Sep-Pak tC18 cartridge (Water Associates, Milford, MA). The adsorbed sample was extracted with 5 mL of DCM as the third extract.

Gas chromatography and mass spectrometry analysis

Identification and quantification of HNOCs within the ACP were conducted using a 7,890 gas chromatograph equipped with a 5,977 mass spectrometer (Agilent Ltd., Santa Clara, CA, United States). Separation was accomplished with an Agilent VF WAX-MS column (30 m × 0.25 mm × 0.25 µm), using the following temperature profile: initial temperature – 50°C, hold – 10 min, 2°C ramp to 160°C, hold – 1 min, 5°C ramp to 240°C, hold – 15 min. Extracted compounds were identified with a NIST 11 mass spectra library (NIST/EPA/NIH mass spectral library, 2011 edition). Standards of 200 ppm 2-pyrrolidinone, pyrazine, and 2-piperidinone in DCM were prepared for quantification. These standards were used to develop a response factor (RF), according to Equation 1. The concentrations of pyrrolidinone, pyrazine, and piperidinone and their alkyl-substituted derivatives ($HNOC_{identified}$) in the samples were then calculated using Equation 2.

$$\textit{Response Factor}\,(RF) = \frac{\textit{Peak Area}_{standard}}{\textit{HNOC}_{concentration}} \quad (1)$$

$$\textit{HNOC Conc.} = \frac{\textit{Peak Area}}{RF} \quad (2)$$

The concentration of each alkyl-substituted derivative was estimated using the response factor of the parent compound. The concentration of each parent compound was summed with the concentrations of its alkyl-substituted derivatives to produce a single concentration for each HNOC group.

Specific ammonia uptake rates

Specific Ammonia Uptake Rate (SAUR) tests were conducted to determine inhibition on autotrophic nitrifiers. The methodology is depicted in Supplementary Figure S1. This assay was performed for 3 pure chemicals (2-pyrrolidinone, pyrazine, and 2-piperidinone) and ACP stored for 1-week and 15-week at five to six different concentrations for each chemical (30 SAUR tests in total). To prevent microbial community changes affecting the results, the activity tests were performed within a single sludge residence time (7 days at the time of experiments).

Return Activated Sludge (RAS) was collected from the KRWWTP on the day of each experiment. At the time of the experiments, the KRWWTP was an aerobic wastewater treatment plant with conventional activated sludge and nitrification (no anaerobic or anoxic zones for biological nitrogen or phosphorus removal). 4L of RAS was aerated for a minimum of 30 min to consume any soluble chemical oxygen demand (sCOD) and remaining nitrite. Excess dissolved oxygen (DO) was provided through diffused-air aeration with a Whisper 300 aerator. DO-limiting conditions were avoided by ensuring a DO value greater than 6 mg L^{-1} measured with YSI OD500 optical probes throughout the SAUR test. Sufficient alkalinity was provided by adding 400 mg L^{-1} as $CaCO_3$ of sodium bicarbonate ($NaHCO_3$) to each batch reactor. The volatile suspended solids (X_{VSS}) concentration was maintained between 2–4 g VSS L^{-1} for each test. Reactor pH was maintained between 7.5 and 8.4 and manually adjusted with 3% HCL solution and $NaHCO_3$. Batch reactors were mixed at 600 rpm with Cole-Parmer overhead impeller mixers model 50,004–00 to ensure sufficient mixing without breaking sludge flocs. 20–40 mg L^{-1}ammonium chloride (NH_4Cl) was fed as excess substrate to begin the test. The inhibitory chemical was added 1 min after the initial SAUR measurement to ensure excess substrate levels were reached. Samples were collected periodically over 3 h. NH_3 was measured with the ammonia phenol method and HACH TNT832 (Rice et al., 2012). The resulting slope of ammonia uptake rate was then calculated and normalized to the respective mixed liquor volatile suspended solids (MLVSS) to obtain a specific rate. The SAUR value was corrected to 20°C according to activated sludge modeling guidelines (Melcer et al., 2003).

IC_{50} toxicity

The 50% inhibitory concentration (IC_{50}) reflects the concentration of a specific HNOC present in the aqueous co-product that inhibited a biological process or response by 50%. The IC_{50} was determined through a four-parameter logistic regression model:

$$SAUR = SAUR_{MIN} + \frac{SAUR_{MAX} - SAUR_{MIN}}{1 + \left(\frac{HNOC}{IC_{50}}\right)^{n}} \quad (3)$$

The model has four key parameters that typically resolve as a sigmoid function (S-shaped curve). For biological inhibition, the Hill coefficient (n) of the equation is positive, indicating a falling steepness of the curve (Sebaugh, 2011). $SAUR_{min}$ is constrained to a positive value to avoid incoherent negative responses in a biological context.

$$SAUR = SAUR_{Min} + \frac{SAUR_{MAX} - SAUR_{Min}}{1 + \left(\frac{HNOC}{IC_{50}}\right)^{n}} \quad (4)$$

$$Fit\ \% = \frac{1 - \sum (SAUR_{measured} - SAUR_{modeled})^2 \Big/ n^{0.5}}{1} \quad (5)$$

The model was then solved for the unknown parameters using Equations 4, 5 for best numerical fit (maximizing % fit) to determine

TABLE 1 Aggregated compounds for each identified HNOC in municipal sludge ACP. Pyrrolidinone, pyrazine, and piperidinone were quantified using standards.

Compound	Peak Area %	Conc (mg/L)
Pyrrolidinone Aggregates		
2-pyrrolidinone, 1-Ethyl-	9.33	317.5
2-Pyrrolidinone, 1-methyl-	9.81	333.9
2-Pyrrolidinone, 1-propyl-	2.18	74.2
2-Pyrrolidinone, 1,5-dimethyl-	1.51	51.2
2-Pyrrolidinone	1.19	40.6
Pyrazine Aggregates		
Pyrazine, methyl-	7.74	225.2
Pyrazine, 2,3-dimethyl-	1.89	55.0
Pyrazine, ethyl-	3.01	87.5
Pyrazine, 2,6-dimethyl-	3.20	93.1
Pyrazine, 2-ethyl-6-methyl-	3.17	92.3
Pyrazine, 3-ethyl-5-methyl-	3.20	93.2
Pyrazine, 3-ethyl-2,5-dimethyl-	2.00	58.3
Pyrazine, 3-ethyl-2,6-dimethyl-	2.41	70.2
Pyrazine, 2,6-diethyl-	0.47	13.7
Pyrazine	1.65	48.0
Piperidinone Aggregates		
2-Piperidinone, 1-methyl-	1.44	48.8
2-Piperidinone	2.51	59.8
Pyridine Aggregates		
Pyridine, 4-methyl-	0.34	
Pyridine, 3-methyl-	1.85	
Pyridine, 2-methyl-	4.40	
Pyridine, 2,6-dimethyl	0.35	
Pyridine, 2,3-dimethyl	0.99	
Pyridine, 1-ethyl	0.38	
Pyridine, 3-ethyl	1.36	
Pyridine	2.68	

10.3389/fceng.2025.1532958

TABLE 2 Quantification of Selected Compounds present in ACP.

Compound	Concentration (ppm)	Concentration (mM)
Pyrrolidinone and derivatives	817	9.60
Pyrazine and derivatives	837	10.4
Piperidinone and derivatives	109	1.10

the hill coefficient (constrained to values between 0 and 5) and 50% inhibitory concentrations.

Results

Identification and quantification of HNOCs in ACP from HTL of municipal sludge

HTL was performed on municipal activated sludge, and an initial qualitative GC-MS analysis was performed on the ACP to select dominant HNOCs for inhibition studies. The identified compounds for this analysis are shown in Table 1. The major HNOCs were pyrrolidinone, pyrazine, piperidinone, and pyridine. These results coincide with previous work from HTL of algal biomass, which determined pyrazine and pyrrolidinone to be the most prevalent HNOCs in the ACP (Alimoradi et al., 2020). Furthermore, piperidinone, pyrrolidinone and pyrazine have been shown to be prevalent in the aqueous phase from HTL of municipal sludge at higher temperatures (Basar et al., 2023). Piperidines are a cyclic compound produced from Maillard reactions between the amino acids and reducing sugars during HTL (Hao et al., 2022; Fan et al., 2023; Basar et al., 2023). Pyrazine and pyridine have similar 6-atom ring chemical structures, with pyridine containing only 1 N atom compared to 2 N atoms in pyrazine. Table 2 shows the relative area and estimated concentrations of pyridine are significantly lower than those of pyrazine. Other organics like phenol, cyclopentene, and alkyl-substituted benzene compounds were also identified but are not the focus of this study.

Based on the preliminary GC-MS results, the compounds selected for individual chemical inhibition tests were, pyrazine, 2-pyrrolidinone, and 2-piperidinone (Figure 2). In the ACP samples, all derivatives with 2-pyrrolidinone, pyrazine, and 2-piperidone as parent compounds were aggregated for quantification. Quantification of the ACP revealed that 2-pyrrolidinone (9.60 mM) and pyrazine (10.4 mM) are present at concentrations ten times higher than 2-piperidinone (1.10 mM) (Table 2).

Inhibition of nitrification by identified HNOCs

To determine the inhibition of nitrifiers by each HNOC, the specific ammonia uptake rate (SAUR) of activated sludge from the KRWWTP was determined with varying concentrations of each chemical. The results with 2-pyrrolidinone are shown in Figure 3, in which SAUR was measured with eight different 2-pyrrolidinone concentrations ranging. Increasing the concentration of 2-pyrrolidinone resulted in a sharp decrease of the SAUR, with SAUR decreasing from 10.8 mg-N/gVSS-hr to 4.1 mg-N/gVSS-hr. The data were fit to the logistic regression model, and the inhibitory concentration expected to reduce ammonia uptake by 50 percent (IC_{50}) was calculated as 5.2×10^{-5} mM with a 94% fit.

The same methodology was performed for the other two model compounds and ACP. Analogous plots for pyrazine and 2-piperidinone can be found in Supplementary Figures S2, S3. Table 3 shows the overall parameters obtained for the logistic regression model of each individual compound. Pyrazine clearly inhibited nitrification, although to a lesser degree than 2-pyrrolidinone. This is reflected by a higher IC_{50} concentration of 2.0×10^{-3} mM with a 97% fit. In contrast, 2-piperidinone did not inhibit nitrification significantly, even at concentrations of 10^{-2} mM. The data were fit into the logistic regression model, but the model resulted in a poor fit with a maximum fit of 31%. Based on the results, 2-piperidinone was determined to not significantly inhibit autotrophic nitrifiers present in activated sludge.

Inhibition of nitrification by the aqueous Co-Product (ACP)

While an understanding of the inhibitory effects of individual HNOCs is important, it is also crucial to determine the inhibitory effect of the ACP, which is a mixture of many compounds, to

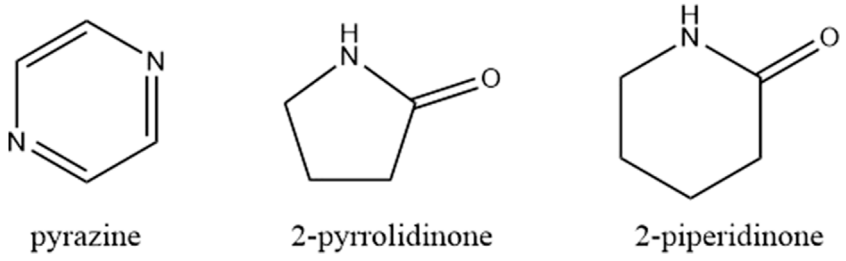

FIGURE 2
Molecular structures of HNOCs selected for individual chemical inhibition tests.

10.3389/fceng.2025.1532958

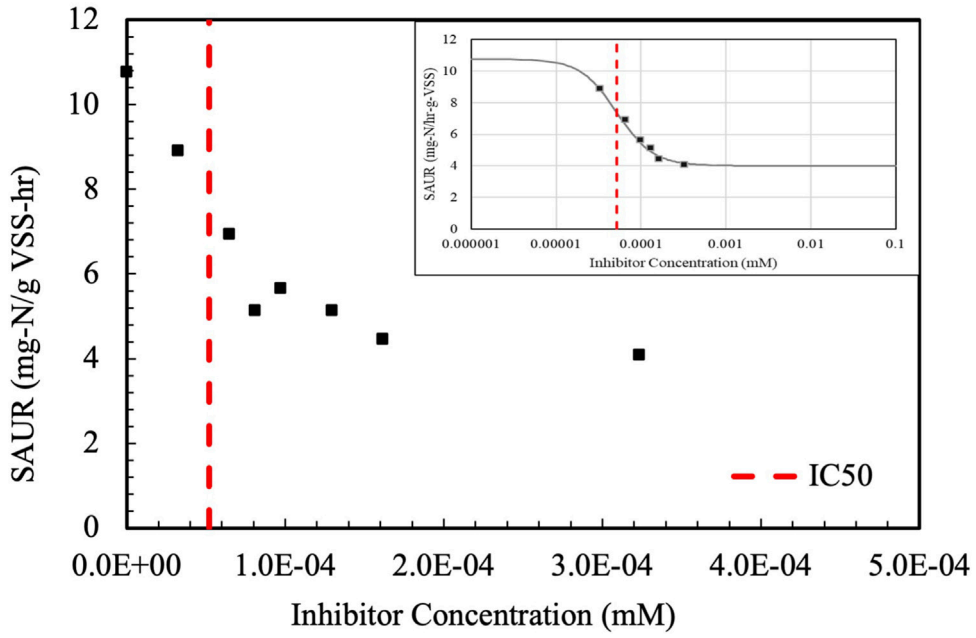

FIGURE 3
2-pyrrolidinone inhibition of specific ammonia uptake rates (SAUR). The logistic regression is shown on the top right. The inhibitory concentration (IC_{50}) is shown in red.

TABLE 3 Inhibition Parameters for each HNOC tested and ACP. IC50 was not observed for 2-piperidinone.

Compound	IC50	Hill Coefficient (n)	SAUR Max (mg-N/g VSS-hr)	SAUR Min (mg-N/g VSS-hr)
2-Pyrrolidinone	5.20×10^{-5} mM	2.0	10.8	4.0
Pyrazine	2.00×10^{-3} mM	1.6	7.4	5.5
2-piperidinone	NA	NA	7.8	6.0
ACP	0.08% (v/v)	3.2	7.8	4.2

nitrification. ACP generated from HTL was stored for 1 week prior to SAUR inhibition testing, and the results are shown in Figure 4. This study is the first to show the inhibitory effect of ACP in activated sludge nitrification with specific ammonia uptake rates going from 7.8 mg-N/gVSS-hr to 3.8 mg-N/gVSS-hr. The data were fit into the logistic regression model, and the IC_{50} was determined to be equal to 0.08% (%v/v). The logistic regression model was maximized to a 74% fit. The dataset does not include as many data points in the plateauing portion of the sinusoidal curve within the model, explaining the lower fit %.

The IC_{50} volumetric ratio corresponds to a 2-pyrrolidinone concentration of 7.52×10^{-3} mM, pyrazine concentration of 5.07×10^{-3} mM, and 2-piperidinone concentration of 3.36×10^{-4} mM (Supplementary Table S1). IC_{50} values of HNOCs within the ACP mixture differed from the inhibitory concentrations for the same compounds when tested individually (Table 3). There are several reasons that individually tested chemicals may exhibit different inhibitory effects than a mixture. Chemicals within a mixture can have antagonistic effects (decreasing the inhibitory effect of individual constituents) or synergistic effects (amplifying inhibitory effects of individual compounds). In this study, 2-pyrrolidinone was more inhibitory as an individual chemical than it appeared within the ACP mixture. However, all compounds that include pyrrolidinone rings were aggregated into a single class of compounds in this study. This may result in overestimating the true concentrations of the compounds.

Effect of ACP Storage Time on Nitrification Inhibition

During initial inhibition studies, it became evident that the ACP color changed over time when stored in the refrigerator for several weeks. To understand the color change and potential chemical changes that could affect inhibition, SAUR experiments were undertaken with ACP stored for 1 week and with ACP stored for 15 weeks post-HTL reaction. The observed color change is shown in Supplementary Figure S3. These tests were performed by increasing the volumetric ratio of the ACP samples and analyzing the % Maximum Activity, which corresponds to the ratio between the SAUR value measured at a specific concentration and the maximum SAUR obtained during the test (Figure 5). In the case of ACP stored for 1 week, the % maximum

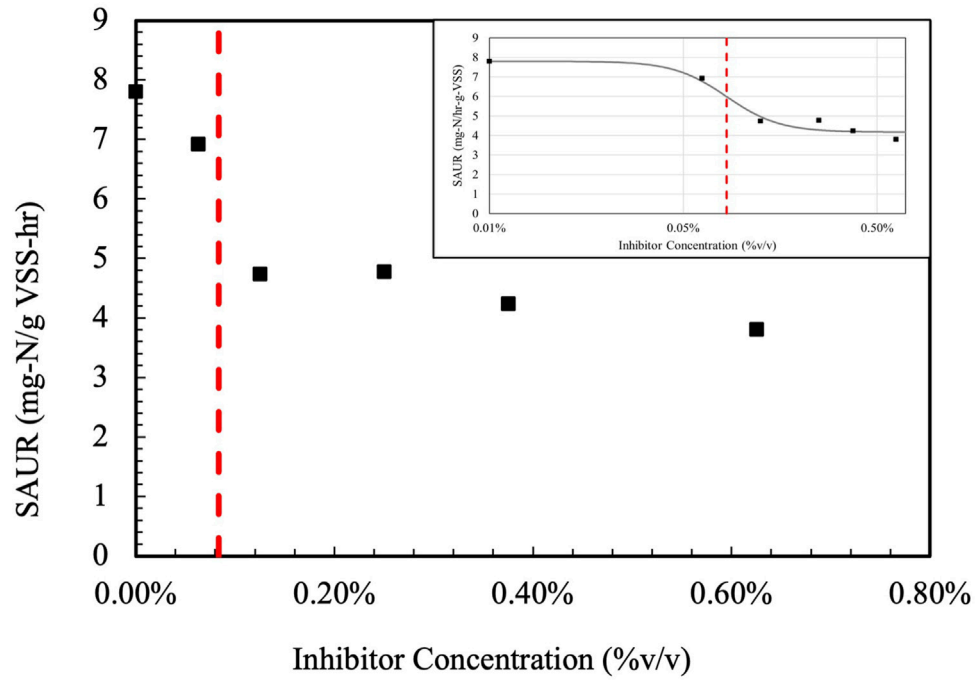

FIGURE 4
ACP inhibition on specific ammonia uptake rates (SAUR). The logistic regression is shown on the top right. The inhibitory concentration (IC_{50}) is shown in red.

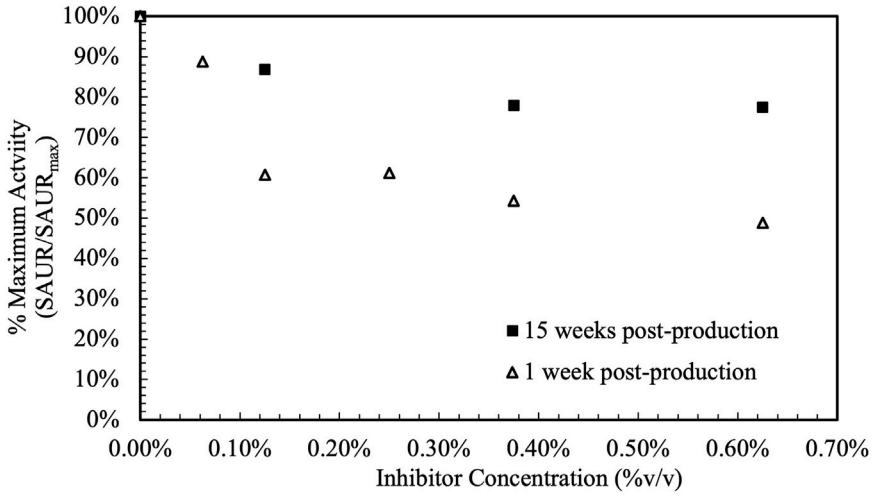

FIGURE 5
Effects of storage time in ACP inhibition of specific ammonia uptake rates (SAUR).

activity was 49% when 0.63% (%v/v) of ACP was added. Conversely, when the same volume of ACP stored for 15 weeks was tested, the % maximum activity only decreased to 77%. These findings suggest that the ACP stored for 15 weeks at 4°C post-HTL reaction had a milder inhibitory effect on the nitrifying community than the ACP stored for 1 week under the same conditions.

The trends observed can be related to chemical changes within the ACP during storage. GC-MS analysis was conducted on samples from both storage conditions (Figure 6; Table 4). The analysis revealed that the overall composition of both samples was similar, with aggregates of pyrazine and 2-pyrrolidinone being the most prevalent HNOCs. The concentrations of N-containing species decreased for pyrazine, 2-pyrrolidinone, and 2-piperidinone from the 1-week storage sample to the fifteen-week storage sample. Specifically, storing ACP for 1 week resulted in total concentrations of 8.22 mM pyrazine, 8.31 mM 2-pyrrolidinone, and 0.96 mM 2-piperidinone aggregates. In contrast, longer storage time led to significant decreases in these compound concentrations, with

10.3389/fceng.2025.1532958

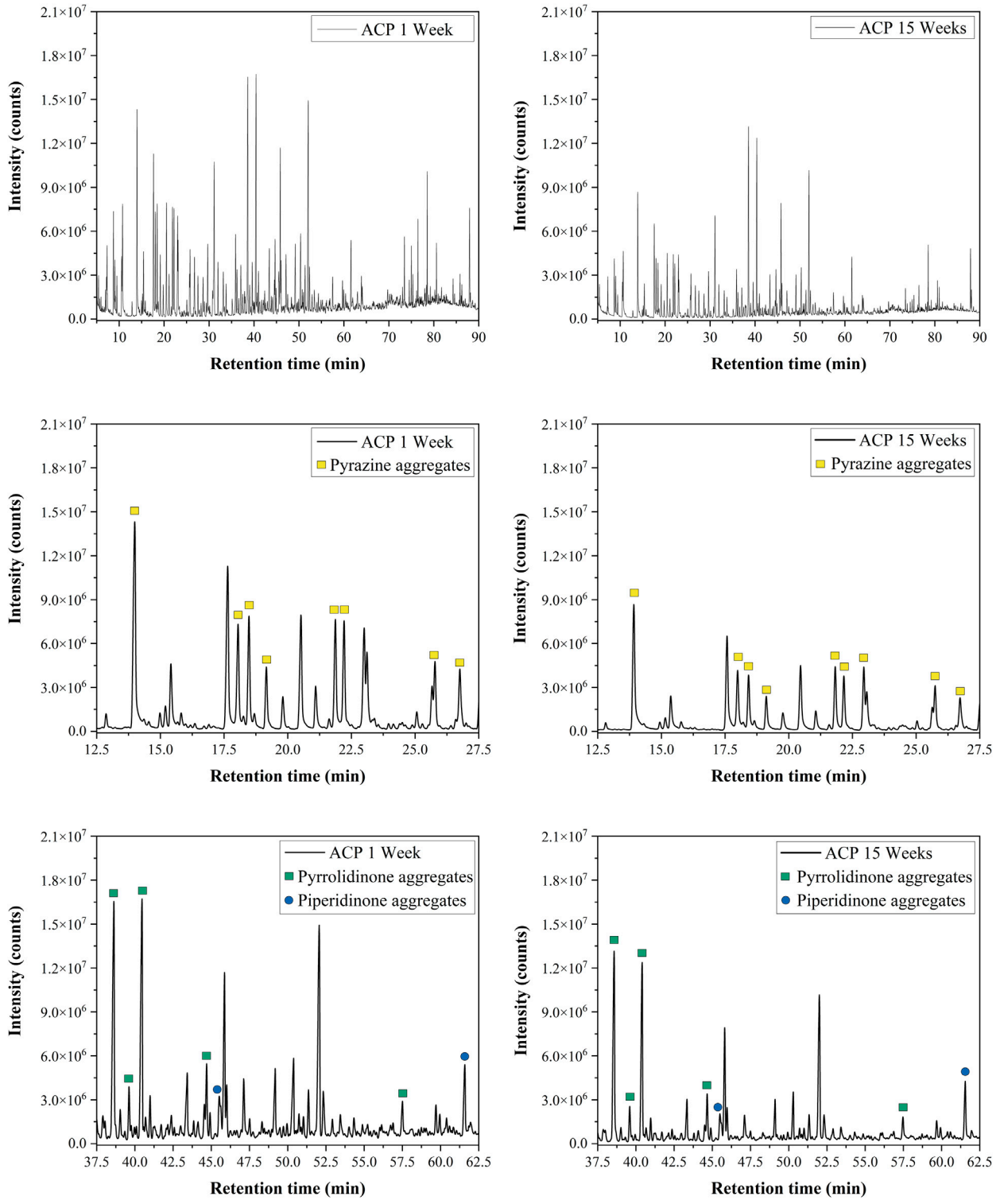

FIGURE 6
GC-MS chromatograms of ACP stored for 1 week and 15 weeks (top row). Pyrazine, pyrrolidinone, and piperidinone compounds are magnified to demonstrate an observed reduction in these compounds during storage.

values of 6.21 mM, 6.36 mM, and 0.85 mM, respectively. These initial findings align with the results from Figure 5, illustrating a reduction in the inhibitory effects of ACP on nitrification over time. While these compounds have been reduced in concentration during ACP storage, other compounds such as phenol and p-cresol significantly increased with the longer storage time. Additional information is necessary to fully comprehend how these chemical changes may contribute to biological inhibition.

10.3389/fceng.2025.1532958

TABLE 4 GC-MS results with the identified compounds in the ACP samples stored during 1 week versus 15 weeks.

Compound	Concentration [mM]	
	1 week storage	15-week storage
pyrazine	0.75	0.43
methylpyrazine	2.59	1.59
2,5-dimethylpyrazine	—	0.87
2,6-dimethylpyrazine	0.90	0.56
ethylpyrazine	0.84	0.46
2,3-dimethylpyrazine	0.53	0.30
2-ethyl-6-methylpyrazine	0.77	0.48
2-ethyl-5-methylpyrazine	0.78	0.39
trimethylpyrazine	—	0.46
2,6-diethylpyrazine	0.11	0.05
3-ethyl-2,5-dimethylpyrazine	0.96	0.49
3,5-diethyl-2-methylpyrazine	—	0.05
2,5-dimethyl-3-(1-propenyl)-pyrazine(Z)	—	0.08
Total Pyrazine Aggregates Conc (mM)	8.22	6.21
1-methyl-2-pyrrolidinone	3.75	3.00
1,5-dimethyl-2-pyrrolidinone	0.48	0.32
1-ethyl-2-pyrrolidinone	3.00	2.02
1-propyl-2-pyrrolidinone	0.60	0.41
2-pyrrolidinone	0.48	0.55
Total Pyrrolidinone Aggregates Conc (mM)	8.31	6.36
1-methyl-2-piperidinone	0.30	0.22
2-piperidinone	0.66	0.63
Total Piperidinone Aggregates (mM)	0.96	0.85

Discussion

Inhibition of nitrification by HNOCs

The inhibitory effects of HNOCs on AOBs and NOBs are largely unknown. A general inhibition mechanism for pyridines was proposed by Prosser et al., suggesting that pyridines are responsible for chelation of the metal components of the ammonia monooxygenase (amo) enzyme, thereby disrupting ammonia oxidation to hydroxylamine in nitrification (Prosser, 1990). Pyrazine is a heterocyclic aromatic compound consisting of a six-membered ring characterized by a pair of nitrogen atoms at positions 1 and 4 on the ring, forming a symmetrically positioned diazine structure (Figure 2). Structurally similar compounds include pyridines, pyrazole, and nitrapyrin. Both nitrapyrin and pyrazole have been found to be inhibitory to nitrification by reducing the abundance of the amoA functional gene in soils (Papadopoulou et al., 2020; Beeckman et al., 2023; Hayden et al., 2021).

Even though there is limited research on the inhibition of pyrazine in nitrifying communities, the use of pyrazine as a corrosion inhibitor may provide insight into the inhibition mechanism. Pyrazine has been studied and utilized as a corrosion inhibitor in steel and other metals, since it binds to the metal surface and inhibits electrochemical processes (Obot and Gasem, 2014; Bouklah et al., 2005). Nitrifiers have been shown to grow rapidly on surfaces like plastic and iron, and at a slower rate on stainless steel (Zhang et al., 2010). While AOBs themselves are not known to be corrosive to steel, the resulting nitrates may indirectly contribute to corrosion under certain conditions. Organic inhibitors like pyrazine provide advantages for corrosion inhibition through formation of chelation layers with the metal surface (Chugh et al., 2020).

HNOCs have been used as coatings for nanoparticles. Silver nanoparticles coated with polyvinyl pyrrolidone have inhibitory effects on nitrifiers *Nitrosomonas europaea*, *Nitrosospira multiformis*, and *Nitrosococcus ocean* (Arnaout and Gunsch, 2012; Beddow et al., 2014). The authors discussed the importance of the nanoparticle coating in cytotoxicity. The inhibitory mechanism of these silver nanoparticles was disruption of the cell wall and cell lysis (Prajitha et al., 2019). Other studies have reported that HNOC inhibition is caused by oxidative stress-related

cell disruption (Macêdo et al., 2023; Papadopoulou et al., 2020; Prosser, 1990).

2-Piperidinone, also known as 2-piperidone, is a heterocyclic organic compound characterized by a piperidine ring, a saturated six-membered ring with one nitrogen atom, fused to a carbonyl group. 2-piperidinone has been identified as an intermediate product of the degradation of pyridine by aerobic bacteria (Feng et al., 1994; Kaiser et al., 1996). In this study, 2-piperidinone was not strongly inhibitory to nitrifiers. However, piperidinone has been shown to have antibacterial activity for heterotrophic gram-positive and gram-negative bacteria (Damayanti and Setyowati, 2020). Further research is necessary to confirm whether 2-piperidinone or pyridine have inhibitory properties for either nitrifiers or heterotrophs in activated sludge.

Inhibition of nitrification by the aqueous Co-Product (ACP)

The overall objective of this study is to determine the inhibitory effects of ACP on activated sludge nitrification. This is necessary to provide guidance on how ACP genereated from HTL at a wastewater treatment plant can be recycled to biological treatment without inhibiting nitrification. In this study, the IC_{50} of ACP was determined to be 0.08% (%v/v). Assuming a wastewater treatment facility would treat the entirety of their WAS with HTL technology, an accurate prediction for sludge production must be done to calculate the ACP generated from HTL. The volumetric ratio of ACP produced to wastewater treated can be compared to the IC_{50} to determine if ACP can be recycled without inhibiting nitrification.

Net WAS production ($P_{x,VSS}$) can be estimated with sufficient wastewater characterization using Equation 6 (Tchobanoglus et al., 2003).

$$P_{x,vss} = \frac{QY\ (S_o - S)\left(10^{-3}\ g/kg\right)}{1 + k_d\,\theta_c} + \frac{(f_d)(k_d)QY\ (S_o - S)(\theta_c)\left(10^{-3}\ g/kg\right)}{1 + k_d\,\theta_c} + \frac{QY_n\ (NO_x)\left(10^{-3}\ g/kg\right)}{1 + k_{dn}\,\theta_c} + Q\,(nbVSS)\ \left(10^{-3}\ g/kg\right) \quad (6)$$

The wastewater characteristics (influent substrate, S_o, of 220 mg L^{-1} and influent ammonia, NO_x, of 24 mg L^{-1}) and treatment goals (effluent substrate, S, or 20 mg L^{-1}) for KRWWTP were used to calculate $P_{x,VSS}$ for a 7-day sludge residence time (θ_c) and a flowrate (Q) of 1 MGD. A range of reference values of sludge yield (Y), nitrifying yield (Yn), decay rate of microorganisms (k_d), decay rate of nitrifying microorganisms (k_{dn}), fraction of cell mass that remains as cell debris (f_d), and non-biodegradable VSS (nbVSS) were used to calculate maximum and minimum sludge production values; these are provided in Supplementary Table S2 (Davis, 2010). The results indicate that the sludge production can range from 139 to 513 kg VSS d^{-1}. Assuming the HTL reaction generates approximately 8 L of ACP per kg VSS, the ACP generated would range from 1,110 – 4100 L d^{-1}.

If all ACP was recycled to the influent of the WWTP, that would represent a percentage ranging from 0.029% – 0.108% (%v/v). This range encompasses the IC_{50} of ACP of 0.08% (%v/v). Based on this estimate, it is possible to recycle ACP generated through HTL of sludge. Optimization of sludge production, ACP yield, and the formation of inhibitory HNOCs can enable recycling of ACP to the biological treatment train. For example, the temperature of the HTL reaction affects HNOC formation (Alimoradi et al., 2020; Basar et al., 2023) and can be optimized to reduce the formation of inhibitory compounds. In this study, storage of ACP was shown to reduce the inhibitory effects to nitrification.

Effect of ACP Storage Time on Nitrification Inhibition

The concentrations of N-containing species decreased for pyrazine, 2-pyrrolidinone, and 2-piperidinone after 14 weeks storage. The mechanism for this degradation is not fully understood, but literature suggests that HNOCs are susceptible to oxidative degradation under aerobic conditions. Studies have shown that pyrazine and similar aromatic heterocycles can undergo oxidation via pathways that include hydroxylation and ring cleavage, facilitated by reactive oxygen species such as hydroxyl radicals or molecular oxygen in the presence of transition metals (Müller and Rappert, 2010). Additionally, compounds like 2-pyrrolidinone and 2-piperidinone, which contain lactam structures, can degrade through hydrolysis or oxidation, resulting in the formation of smaller, less inhibitory molecules, such as carboxylic acids or amines (Smith, 2011). These transformations may be further promoted by trace catalytic components such as iron or manganese, which are commonly present in the ACP matrix (Burroughs et al., 2019). At full-scale, ACP could be stored prior to recycling to biological treatment to reduce the concentration of inhibitory compounds, or an advanced oxidation system. Further research is needed to understand the mechanism to HNOC reduction, so the process can be optimized.

Impact of microbial community structure on IC_{50}

The SAUR assays were performed throughout January and April, with activated sludge harvested from a full-scale nitrification WWTP during these months. During the January experiments, the water temperature was 12°C, and nitrification was performing well. However, nitrifiers are slow-growing organisms, and growth is dependent on temperature. At full-scale, nitrification failures have been documented during colder seasons (Johnston et al., 2023; Johnston et al., 2019; Kim et al., 2006). At low temperatures, nitrifiers may be washed out if sludge residence times are not sufficiently maintained. Even when AOBs are abundant, they may lower their amoA gene expression at cold temperatures (Johnston et al., 2023). In this study, the AUR were corrected for temperature and normalized to total biomass concentrations (VSS), but the inhibitory impact of HNOCs could be magnified due to changes in the nitrifier community cultivated at low temperatures. The nitrifier fraction in VSS will also change seasonally. A more robust and abundant nitrifying community during the summer may exhibit less inhibitory effects.

Conclusion

HTL presents an innovative approach to energy recovery from municipal sludge, offering a unique set of advantages in the context of wastewater treatment. HTL addresses the challenge of sludge management by transforming the organic content into a valuable energy resource. Incorporating HTL for sludge processing and recycling the ACP presents a promising avenue for sustainable wastewater treatment practices. The toxicity of HNOCs and their effects on heterothrophic bacteria has been investigated in previous works. The present study showed the inhibitory effects of HNOCs to autotrophic nitrifiers and calculated the IC_{50} for three individual HNOCs and ACP.

GC-MS analysis of ACP generated from HTL of municipal sludge determined 2-pyrrolidinone and pyrazine and their derivatives as the most prevalent HNOCs at concentrations of 8.98 and 0.40 mM respectively. These compounds were shown to be inhibitory to nitrifying bacteria with IC_{50} values of 5.2×10^{-5} mM for 2-pyrrolidinone and 2.0×10^{-3} mM for pyrazine. 2-piperidinone was not found to be strongly inhibitory to nitrification. The IC_{50} of the ACP was 0.08% (%v/v) for an ACP sample stored 1-week after production. This corresponded to concentrations of 2-pyrrolidinone, pyrazine, and 2-piperidinone of 7.52×10^{-3}, 5.07×10^{-3}, and 3.36×10^{-4} mM respectively.

The volumetric ACP production from municipal sludge HTL was estimated. If all ACP was recycled to the influent of the WWTP, that would represent a percentage ranging from 0.026% – 0.098% (% v/v). This range encompasses the IC_{50} of ACP of 0.08% (%v/v). Based on this estimate, it is possible to recycle ACP generated through HTL of sludge. Storage of ACP can be used to reduce the concentration of inhibitory HNOCs. GC-MS data showed that the overall concentration of the three selected HNOCs in this study were reduced with 15 weeks of ACP storage.

This study demonstrates that ACP generated from HTL of municipal sludge can be recycled within the WWTP, which is a key factor for full-scale implementation of HTL. The feasibility of HTL as a solids processing technology is enhanced by promoting resource recovery and minimizing environmental impacts.

Data availability statement

The original contributions presented in the study are included in the article/Supplementary Material, further inquiries can be directed to the corresponding author.

Author contributions

AR: Data curation, Formal Analysis, Investigation, Visualization, Writing–original draft. JP: Data curation, Formal Analysis, Investigation, Visualization, Writing–review and editing. SL: Investigation, Writing–review and editing. SS-W: Conceptualization, Resources, Supervision, Validation, Writing–review and editing. RC: Methodology, Validation, Writing–review and editing. BS: Conceptualization, Data curation, Funding acquisition, Methodology, Project administration, Resources, Supervision, Validation, Writing–review and editing.

Funding

The author(s) declare financial support was received for the research, authorship, and/or publication of this article. The authors acknowledge the University of Kansas School of Engineering for providing support for Romero and Poli and the University of Kansas Office of Research for providing support for Larson.

Acknowledgments

The authors acknowledge the City of Lawrence for providing activated sludge for the HTL reactions and inhibitory SAUR assays.

Conflict of interest

The authors declare that the research was conducted in the absence of any commercial or financial relationships that could be construed as a potential conflict of interest.

Generative AI statement

The author(s) declare that no Generative AI was used in the creation of this manuscript.

Publisher's note

Supplementary material

The Supplementary Material for this article can be found online at: https://www.frontiersin.org/articles/10.3389/fceng.2025.1532958/full#supplementary-material

References

Adedeji, O. M., Bauer, S. K., and Jahan, K. (2023). Anaerobic digestion of aqueous product of co-hydrothermal liquefaction of beverage waste and sewage sludge: reduction of toxicity and energy assessment. *Energy Convers. Manag.* 290, 117228. doi:10.1016/j.enconman.2023.117228

Alimoradi, S., Stohr, H., Stagg-Williams, S., and Sturm, B. (2020). Effect of temperature on toxicity and biodegradability of dissolved organic nitrogen formed during hydrothermal liquefaction of biomass. *Chemosphere* 238, 124573. doi:10.1016/j.chemosphere.2019.124573

Arnaout, C. L., and Gunsch, C. K. (2012). Impacts of silver nanoparticle coating on the nitrification potential of Nitrosomonas europaea. *Environ. Sci. and Technol.* 46, 5387–5395. doi:10.1021/es204540z

Basar, I. A., Liu, H., and Eskicioglu, C. (2023). Incorporating hydrothermal liquefaction into wastewater treatment–Part III: aqueous phase characterization and evaluation of on-site treatment. *Chem. Eng. J.* 467, 143422. doi:10.1016/j.cej.2023.143422

Beddow, J., Stolpe, B., Cole, P., Lead, J. R., Sapp, M., Lyons, B. P., et al. (2014). Effects of engineered silver nanoparticles on the growth and activity of ecologically important microbes. *Environ. Microbiol. Rep.* 6, 448–458. doi:10.1111/1758-2229.12147

Beeckman, F., Drozdzecki, A., De Knijf, A., Corrochano-Monsalve, M., Bodé, S., Blom, P., et al. (2023). Drug discovery-based approach identifies new nitrification inhibitors. *J. Environ. Manag.* 346, 118996. doi:10.1016/j.jenvman.2023.118996

Bouklah, M., Attayibat, A., Kertit, S., Ramdani, A., and Hammouti, B. (2005). A pyrazine derivative as corrosion inhibitor for steel in sulphuric acid solution. *Appl. Surf. Sci.* 242, 399–406. doi:10.1016/j.apsusc.2004.09.005

Burroughs, A. M., Glasner, M. E., Barry, K. P., Taylor, E. A., and Aravind, L. (2019). Oxidative opening of the aromatic ring: tracing the natural history of a large superfamily of dioxygenase domains and their relatives. *J. Biol. Chem.* 294, 10211–10235. doi:10.1074/jbc.ra119.007595

Chen, H., Hao, S., Chen, Z., Sompong, O., Fan, J., Clark, J., et al. (2020). Mesophilic and thermophilic anaerobic digestion of aqueous phase generated from hydrothermal liquefaction of cornstalk: molecular and metabolic insights. *Water Res.* 168, 115199. doi:10.1016/j.watres.2019.115199

Chugh, B., Singh, A. K., Chaouiki, A., Salghi, R., Thakur, S., and Pani, B. (2020). A comprehensive study about anti-corrosion behaviour of pyrazine carbohydrazide: gravimetric, electrochemical, surface and theoretical study. *J. Mol. Liq.* 299, 112160. doi:10.1016/j.molliq.2019.112160

Damayanti, P. N., and Setyowati, E. P. (2020). Synthesis and antibacterial activity of 4-Piperidone curcumin analogues against Gram-positive and Gram-negative bacteria. *Res. J. Pharm. Technol.* 13, 4765–4769. doi:10.5958/0974-360x.2020.00838.0

Davis, M. L. (2010). *Water and wastewater engineering: design principles and practice*. McGraw-Hill.

Fan, Y., Meyer, L., Gong, M., Krause, B., Hornung, U., and Dahmen, N. (2023). Understanding the fate of nitrogen during catalytic hydrothermal liquefaction of sewage sludge. *Fuel* 339, 126948. doi:10.1016/j.fuel.2022.126948

Feng, Y., Kaiser, J.-P., Minard, R. D., and Bollag, J.-M. (1994). Microbial transformation of ethylpyridines. *Biodegradation* 5, 121–128. doi:10.1007/bf00700637

Gu, Y., Zhang, X., Deal, B., and Han, L. (2019). Biological systems for treatment and valorization of wastewater generated from hydrothermal liquefaction of biomass and systems thinking: a review. *Bioresour. Technol.* 278, 329–345. doi:10.1016/j.biortech.2019.01.127

Hable, R. D., Alimoradi, S., Sturm, B. S., and Stagg-Williams, S. M. (2019). Simultaneous solid and biocrude product transformations from the hydrothermal treatment of high pH-induced flocculated algae at varying Ca concentrations. *Algal Res.* 40, 101501. doi:10.1016/j.algal.2019.101501

Hao, B., Yang, W., Wang, Y., Xu, D., Kapusta, K., and Guo, Y. (2022). Hydrothermal liquefaction of municipal sludge: coupling effects of temperature and time on nitrogen migration. *J. Anal. Appl. Pyrolysis* 165, 105562. doi:10.1016/j.jaap.2022.105562

Hayden, H. L., Phillips, L. A., Marshall, A. J., Condon, J. R., Doran, G. S., Wells, G. S., et al. (2021). Nitrapyrin reduced ammonia oxidation with different impacts on the abundance of bacterial and archaeal ammonia oxidisers in four agricultural soils. *Appl. Soil Ecol.* 157, 103759. doi:10.1016/j.apsoil.2020.103759

He, Y., Li, X., Xue, X., Swita, M. S., Schmidt, A. J., and Yang, B. (2017). Biological conversion of the aqueous wastes from hydrothermal liquefaction of algae and pine wood by Rhodococci. *Bioresour. Technol.* 224, 457–464. doi:10.1016/j.biortech.2016.10.059

Johnston, J., du, Z., and Behrens, S. (2023). Ammonia-oxidizing bacteria maintain abundance but lower amoA-gene expression during cold temperature nitrification failure in a full-scale municipal wastewater treatment plant. *Microbiol. Spectr.* 11, e025712222. doi:10.1128/spectrum.02571-22

Johnston, J., Lapara, T., and Behrens, S. (2019). Composition and dynamics of the activated sludge microbiome during seasonal nitrification failure. *Sci. Rep.* 9, 4565. doi:10.1038/s41598-019-40872-4

Kaiser, J.-P., Feng, Y., and Bollag, J.-M. (1996). Microbial metabolism of pyridine, quinoline, acridine, and their derivatives under aerobic and anaerobic conditions. *Microbiol. Rev.* 60, 483–498. doi:10.1128/mr.60.3.483-498.1996

Kim, D.-J., Lee, D.-I., and Keller, J. (2006). Effect of temperature and free ammonia on nitrification and nitrite accumulation in landfill leachate and analysis of its nitrifying bacterial community by FISH. *Bioresour. Technol.* 97, 459–468. doi:10.1016/j.biortech.2005.03.032

Li, R., Liu, D., Zhang, Y., Tommaso, G., Si, B., Liu, Z., et al. (2022). Enhanced anaerobic digestion of post-hydrothermal liquefaction wastewater: bio-methane production, carbon distribution and microbial metabolism. *Sci. Total Environ.* 837, 155659. doi:10.1016/j.scitotenv.2022.155659

Li, Y., Tarpeh, W. A., Nelson, K. L., and Strathmann, T. J. (2018). Quantitative evaluation of an integrated system for valorization of wastewater algae as bio-oil, fuel gas, and fertilizer products. *Environ. Sci. and Technol.* 52, 12717–12727. doi:10.1021/acs.est.8b04035

Macêdo, W. V., Schmidt, J. S., Jensen, S. B., Biller, P., and Vergeynst, L. (2023). Is nitrification inhibition the bottleneck of integrating hydrothermal liquefaction in wastewater treatment plants? *J. Environ. Manag.* 348, 119046. doi:10.1016/j.jenvman.2023.119046

Melcer, H., Dold, P. L., Jones, R. M., Bye, C. M., Takacs, I., Stensel, H. D., et al. (2003). Methods for wastewater characterization in activated sludge modelling. Available at: https://www.waterrf.org/research/projects/methods-wastewater-characterization-activated-sludge-modeling.

Mulchandani, A., and Westerhoff, P. (2016). Recovery opportunities for metals and energy from sewage sludges. *Bioresour. Technol.* 215, 215–226. doi:10.1016/j.biortech.2016.03.075

Müller, R., and Rappert, S. (2010). Pyrazines: occurrence, formation and biodegradation. *Appl. Microbiol. Biotechnol.* 85, 1315–1320. doi:10.1007/s00253-009-2362-4

Obot, I., and Gasem, Z. (2014). Theoretical evaluation of corrosion inhibition performance of some pyrazine derivatives. *Corros. Sci.* 83, 359–366. doi:10.1016/j.corsci.2014.03.008

Padoley, K., Mudliar, S., and Pandey, R. (2008). Heterocyclic nitrogenous pollutants in the environment and their treatment options–an overview. *Bioresour. Technol.* 99, 4029–4043. doi:10.1016/j.biortech.2007.01.047

Papadopoulou, E. S., Bachtsevani, E., Lampronikou, E., Adamou, E., Katsaouni, A., Vasileiadis, S., et al. (2020). Comparison of novel and established nitrification inhibitors relevant to agriculture on soil ammonia-and nitrite-oxidizing isolates. *Front. Microbiol.* 11, 581283. doi:10.3389/fmicb.2020.581283

Peccia, J., and Westerhoff, P. (2015). We should expect more out of our sewage sludge. *Environ. Sci. Technol.* 49 (14), 8271–8276.

Pham, M., Schideman, L., Scott, J., Rajagopalan, N., and Plewa, M. J. (2013). Chemical and biological characterization of wastewater generated from hydrothermal liquefaction of Spirulina. *Environ. Sci. and Technol.* 47, 2131–2138. doi:10.1021/es304532c

Prajitha, N., Athira, S., and Mohanan, P. (2019). Bio-interactions and risks of engineered nanoparticles. *Environ. Res.* 172, 98–108. doi:10.1016/j.envres.2019.02.003

Prosser, J. (1990). Autotrophic nitrification in bacteria. *Adv. Microb. physiology* 30, 125–181. doi:10.1016/s0065-2911(08)60112-5

Rice, E. W., Bridgewater, L., and Association, A. P. H. (2012). *Standard methods for the examination of water and wastewater*. Washington, DC: American public health association.

Rittmann, B. E., Mayer, B., Westerhoff, P., and Edwards, M. (2011). Capturing the lost phosphorus. *Chemosphere* 84, 846–853. doi:10.1016/j.chemosphere.2011.02.001

Roberts, G. W., Fortier, M.-O. P., Sturm, B. S., and Stagg-Williams, S. M. (2013). Promising pathway for algal biofuels through wastewater cultivation and hydrothermal conversion. *Energy and Fuels* 27, 857–867. doi:10.1021/ef3020603

Sebaugh, J. (2011). Guidelines for accurate EC50/IC50 estimation. *Pharm. Stat.* 10, 128–134. doi:10.1002/pst.426

Smith, J. G. (2011). *Organic chemistry*. McGraw-Hill.

Tarallo, S. (2014). *Utilities of the future energy findings*. IWA Publishing. doi:10.2166/9781780406800

Tchobanoglus, G., Burton, F., and Stensel, H. D. (2003). *Wastewater engineering: treatment and reuse*. McGraw-Hill: Boston.

Thomsen, L. B. S., Anastasakis, K., and Biller, P. (2022). Wet oxidation of aqueous phase from hydrothermal liquefaction of sewage sludge. *Water Res.* 209, 117863. doi:10.1016/j.watres.2021.117863

Watson, J., Wang, T., Si, B., Chen, W.-T., Aierzhati, A., and Zhang, Y. (2020). Valorization of hydrothermal liquefaction aqueous phase: pathways towards commercial viability. *Prog. Energy Combust. Sci.* 77, 100819. doi:10.1016/j.pecs.2019.100819

Wu, B., Berg, S. M., Remucal, C. K., and Strathmann, T. J. (2020). Evolution of N-containing compounds during hydrothermal liquefaction of sewage sludge. *ACS Sustain. Chem. and Eng.* 8, 18303–18313. doi:10.1021/acssuschemeng.0c07060

Xu, D., Liu, L., Wei, N., Guo, Y., Wang, S., Wu, Z., et al. (2019). Catalytic supercritical water gasification of aqueous phase directly derived from microalgae hydrothermal liquefaction. *Int. J. Hydrogen Energy* 44, 26181–26192. doi:10.1016/j.ijhydene.2019.08.106

Zhang, Y., Griffin, A., and Edwards, M. (2010). Effect of nitrification on corrosion of galvanized iron, copper, and concrete. *Journal-American Water Works Assoc.* 102, 83–93. doi:10.1002/j.1551-8833.2010.tb10093.x

Zhou, M., Yan, B., Wong, J. W., and Zhang, Y. (2018). Enhanced volatile fatty acids production from anaerobic fermentation of food waste: a mini-review focusing on acidogenic metabolic pathways. *Bioresour. Technol.* 248, 68–78. doi:10.1016/j.biortech.2017.06.121